Theoretical Consideration of Experimental Methods for X-ray Phase Determination Using Multiple Diffraction

By Shih-Lin Chang*

Max-Planck-Institut für Festkörperforschung, Heisenbergstrasse 1, 7000 Stuttgart 80, Federal Republic of Germany

Abstract

Previously reported experimental methods for X-ray phase determination are analyzed using the plane-wave dynamical theory of X-ray diffraction. The relation between the dispersion surface and the phases are considered as well as the influence of the crystal rotation relative to the Ewald sphere on the diffraction line profile. It is shown that the phase information obtained from the intensity of three-beam Borrmann diffraction may get lost due to crystal thickness effects. Three-beam Bragg reflections, either *Umweg* or *Aufhellung*, give optimal conditions to reveal the phases, provided that the relative rotation of the additional reciprocal-lattice point entering or leaving the Ewald sphere is known. With the exception of special situations, N-beam cases with $N > 3$ are found not to be suitable for phase determination, since they involve high-order phase products and thus complicate the experimental determination of the phases.

1. Introduction

The experimental determination of X-ray reflection phases, the so-called 'X-ray phase problem', is one of the unsolved problems in crystallography as well as in X-ray physics. The difficulties in solving this problem result from the fact that the phase information is lost in two-beam diffraction (Ewald & Heno, 1968).

In contrast to X-rays, the reflection phases of visible light are easily determined by the interference of two coherent beams coming from a single source or a pair sources, though the difficulties still exist. Optical holography is a well known example for using the phase contrast of two coherent beams, an incident beam and a reference beam.

The coherent dynamical interaction in X-ray multiple diffraction has long been considered to provide clues for phase determination (Lipscomb, 1949; Eckstein, 1949; Fankuchen, 1949). X-ray multiple diffrac-

* On leave from Instituto de Física, Universidade Estadual de Campinas, Campinas, SP 13100, Brazil.

tion is analogous to optical holography, since one of the diffracted X-ray beams can be treated as a reference for the other beam. The relative phase difference between the two beams modifies the diffracted intensity of the reference beam. Phase information could therefore be extracted from the intensity variation on the reference beam. Efforts have been made, for instance, by using a three-beam *Pendellösung* effect (Hart & Lang, 1961), three-beam Borrmann diffraction (Post, 1977), two overlapped three-beam *Umweganregungen* treated as a four-beam case (Chapman, Yoder & Colella, 1981) and four- and five-beam diffractions (Jagodzinski, 1980). Similar investigations have also been carried out for electron diffraction, for example, by Kambe & Miyake (1954), Miyake & Kambe (1954), Kambe (1957), Berndt & Doll (1976), and Madsen & Cotterill (1978). All these X-ray experiments involve directly or indirectly the rotation of the crystal lattice relative to the Ewald sphere. However, the influence of sense of this rotation with additional reciprocal-lattice point entering (incoming) or leaving (outgoing) the Ewald sphere on the diffracted intensity has never been considered explicitly.

Recently, Chang (1981, 1982) pointed out that the three-beam multiple-reflected intensity profile depends not only on the sign, $S_{P,T}$, of the triplet phase product, but also on the sense of the crystal rotation, either incoming or outgoing. For centrosymmetric structures, the sign $S_{P,T}$ is defined as

$$S_{P,T} = S_{-H_1} S_{H_2} S_{H_1-H_2}, \qquad (1)$$

where S_{-H_1}, S_{H_2}, and $S_{H_1-H_2}$ are the signs of the structure factors of $-H_1$, H_2, and $H_1 - H_2$ reflections. Here H_1 is a symmetric Bragg reflection, the so-called primary reflection (Renninger, 1937; Moon & Shull, 1964). H_2 is the additional reflection (the secondary reflection). The interaction reflection between H_1 and H_2 is $H_1 - H_2$. A useful relation between $S_{P,T}$, the sign S_L defined from diffraction line profiles, and the sense of rotation S_R is established (Chang, 1981, 1982) for experimental determination of the phases. Demonstration of this method in combination with the ordinary 'direct method' of structure determination has

been carried out on a conventional four-circle single-crystal diffractometer (Chang & Han, 1982).

The purpose of this paper is to give an analysis to all of the present suggested experimental methods for phase determination using X-ray multiple diffraction, on the basis of the dynamical theory of X-ray diffraction. The justification and applicability of these methods are discussed.

2. Dynamical theory for N-beam ($N > 2$) diffraction

According to dynamical theory, X-ray reflection phases are always involved in the wavefields generated in crystals. N-beam ($N > 2$) dynamical diffractions are most suitable for meaningful phase determination, since the phase products of reflection sets whose vectors form a closed loop are independent of the choice of origin of the crystal unit cell. The dynamical theory of X-ray diffraction is needed for describing the wavefields and hence for extracting the phase information from the N-beam interaction.

The self-consistent two-beam dynamical theory was first derived by Ewald (1916a,b, 1917, 1937) and modified by von Laue (1931), then generalized for N-beam cases by Kato (1958). Fairly complete references in relation to this subject can be found in the articles by von Laue (1960), James (1963), Batterman & Cole (1964), Kato (1974), Pinsker (1978), and Schwartz & Cohen (1977). Although there are different approaches (Colella, 1974; Kohn, 1979) for N-beam diffraction, we shall follow von Laue's (1931) treatment, which is most commonly used for N-beam dynamical calculation.

In dynamical theory, diffraction of X-rays is described by Maxwell's equations for a medium with a periodic, complex dielectric constant. The solution of the equations, the wave field $\mathbf{D}$, is assumed as a superposition of Bloch waves which satisfy Bragg's law, $i.e.$

$$\mathbf{D} = \sum_H \mathbf{D}_H \exp\{-2\pi i(\mathbf{K}_H \cdot \mathbf{r} - vt)\}, \qquad (2)$$

where $\mathbf{K}_H = \mathbf{K}_0 + \mathbf{H}$. The vector $\mathbf{H}$ represents the reciprocal-lattice vector of H reflection. $\mathbf{K}_0$ and $\mathbf{K}_H$ are the wave vectors of the incident beam 0 and the reflected beam H in the crystal. $\mathbf{D}_H$ is the dielectric displacement of the reflected beam H.

The fundamental equation of the wavefield is derived from the solution of Maxwell's equations for each diffracted beam as

$$2\varepsilon_H \mathbf{D}_H = \sum_{H'} \Phi_{H-H'} \mathbf{D}_{H'[H]}, \qquad (3)$$

where

$$2\varepsilon_H = (\mathbf{K}_H \cdot \mathbf{K}_H)/k^2 - 1, \qquad (4)$$

$$\Phi_{H-H'} = (e^2/mc^2)(\lambda^2/\pi V) F_{H-H'} \equiv F_{H-H'}/\gamma. \qquad (5)$$

$F_{H-H'}$ is the structure factor for the $H - H'$ reflection. $D_{H'[H]}$ is the vector component of $\mathbf{D}_H$ perpendicular to $\mathbf{K}_H$. k is equal to $1/\lambda$, where λ is the vacuum wavelength of the X-ray used. e and m are the charge and mass of the electron. The vacuum velocity of light is c. The volume of the unit cell is V. The sum in (3) is taken over N reflections, $i.e.$ 0, H, ..., and Q.

Equation (3) involves $2N$ linear equations, when the polarization is considered. For simplicity and without losing significantly the generality, we will ignore the polarization. By combining (3) and (5), the fundamental equation of the wavefield becomes

$$\begin{pmatrix} F_0 - 2\varepsilon_0\gamma & F_{-H} & \cdots & F_{-Q} \\ F_H & F_0 - 2\varepsilon_0\gamma & \cdots & F_{H-Q} \\ \vdots & \vdots & \ddots & \vdots \\ F_Q & F_{Q-H} & \cdots & F_0 - 2\varepsilon_0\gamma \end{pmatrix} \begin{pmatrix} D_0 \\ D_H \\ \vdots \\ D_Q \end{pmatrix} = 0.$$

$$(6)$$

Equation (6) can be easily solved as a complex eigenvalue equation. The real parts of the eigenvalues yield the positions of the tie points (Ewald, 1917) on the N sheets of the dispersion surface. The imaginary parts determine the absorption coefficients. The corresponding eigenvectors give the ratios of the wavefield amplitudes between the diffracted and the incident beams. Each eigenvalue defines a type of wave propagation within the crystal, the so-called mode of propagation (Saccocio & Zajac, 1965). According to Pinsker (1978, p. 478) and Chang (1979), the total number, N_{eff}, of effective modes involved in an N beam diffraction is $N_{eff} = N - N_{Bragg}$ for a thick crystal with about $\mu t > 10$, where μ and t are the linear absorption coefficient and the crystal thickness. N_{Bragg} is the number of Bragg reflections involved. For thin crystals, N modes must be considered.

The normal components of the dielectric displacement and the tangential components of the electric and magnetic fields must be continuous at the crystal boundary to determine the wavefield amplitudes D_0, D_H, ... and D_Q. However, the dielectric susceptibility is of the order of 10^{-5} for X-rays; therefore, the boundary conditions can be replaced: the electric fields E in vacuum equal the dielectric displacements D inside the crystal (Kato, 1974). This implies that

$$\sum_j D_0(j) = E_0,$$

$$\sum_j D_T(j) = 0, \text{ for each transmitted beam } T, \qquad (7)$$

$$\sum_j D_R(j) = E_R, \text{ for each reflected beam } R.$$

The summations are taken over the effective modes. The subscripts 0, T, and R indicate the direct incident, the transmitted, and the reflected beams, respectively. Setting E_0 equal to unity yields the reflected and transmitted intensities

$$I_R = |E_R|^2 \qquad (8)$$

and

$$I_T(\mathbf{r}) = \left(\sum_j \{D_T(j) \exp[-2\pi i \mathbf{K}_T'(j) \cdot \mathbf{r}] \right.$$
$$\left. \times \exp[-2\pi \mathbf{K}_T''(j) \cdot \mathbf{r}]\} \right)^2, \qquad (9)$$

where $\mathbf{K}_T = \mathbf{K}_T' - i\mathbf{K}_T''$.

For an unpolarized incident beam the correlation between the crystal excitation by the σ component of the incident wave (perpendicular to the two-beam plane of incidence) and by the π component (parallel to the plane of incidence) must be included in (7), (8) and (9). It is however a formidable task to obtain an analytical expression for the phase dependence of the diffracted intensities in M-beam cases. An attempt has been given by Ewald & Heno (1968). Explicit mathematical relations between the diffracted intensity and phases have not been obtained.

The dispersion surface usually contains the information about the phases. Therefore, we will discuss in the following the relation between the phases and the dispersion surface in connection with the experimental methods for phase determination.

3. Experimental methods for phase determination

(a) Three-beam Borrmann diffraction

For three-beam, 0, H and H', Borrmann diffraction the dispersion surface can be described by the following equation:

$$\chi^3 - (F_H^2 + F_{H'}^2 + F_{H-H'}^2)\chi$$
$$+ 2|F_{-H}F_{H'}F_{H-H'}| \cos \beta = 0, \qquad (10)$$

with

$$S_{P,T} = \cos \beta,$$

where $\chi = F_0 - 2\varepsilon_0 \gamma$. Equation (10) determines three values of χ corresponding to three dispersion sheets. It has been shown (Post, 1977) that the location of these three dispersion sheets depends on the sign $S_{P,T}$, namely the invariant phast angle β of the structure factor triplet $F_{-H}F_{H'}F_{H-H'}$. For a positive $S_{P,T}$, two of the three dispersion sheets are closer to the Laue point. For a negative $S_{P,T}$ two sheets are at positions away from the Laue point. Similar arguments have been given by Kambe (1957).

Dispersion surface is a characteristic for a given reflection, radiation and crystal. The dispersion surface is the same for both (Laue) transmission and (Bragg) reflection, except that the entrance crystal surface relative to the X-ray beams is different. The entrance crystal surface is parallel and perpendicular to the reciprocal-lattice vector, for a symmetric Laue and a symmetric Bragg reflection, respectively.

The intersection of the dispersion surface with the plane of incidence of the H reflection is shown schematically in Fig. 1(a). The relation between the dispersion sheets and the angular deviation, $\Delta\theta$, from the Bragg angle θ of H reflection is seen. La and Lo are Laue and Lorentz points respectively. Branches 1 and 2 are the distorted two-beam dispersion sheets of the H reflection. For a positive $S_{P,T}$, the third dispersion sheet (branch 3^+) lies in between Lo and branch 1. For a negative $S_{P,T}$, the third branch, 3^-, lies in between Lo and branch 2.

The excitation of tie points by the incident wave is determined by the line normal to the crystal surface from the entrance points to fulfill the continuity of the tangential components of the wave vectors inside and outside the crystal at the crystal boundary. For a positive $S_{P,T}$ and $\Delta\theta < 0$, three tie points, R_1, R_2, and R_3, are excited. Since the Poynting vectors at R_1 and R_2 perpendicular to the corresponding dispersion sheets (Kato, 1958) point towards the direction of the incident beam, $i.e.$ along LaO, these two modes associated with R_1 and R_2 are more strongly excited than the mode at R_3. For $\Delta\theta > 0$, T_2 and T_3 are more excited than T_1. Similar situations occur at the crystal settings which are off the exact three-beam diffraction point ($\varphi = 0$). The angle φ is the azimuthal rotation angle of the third reciprocal-lattice point H' around $0H$. The projection of Fig. 1(a) on the plane perpendicular to and bisecting $0H$ is shown in Fig. 1(b). For $\varphi < 0$, tie points X_1 and X_2 are more excited than X_2. For $\varphi > 0$, Y_2 and Y_3 are
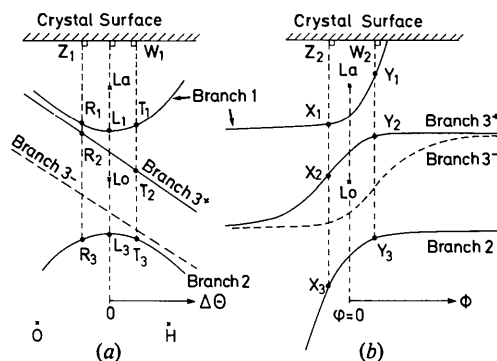

Fig. 1. Schematic representation of the dispersion surface for symmetric three-beam, 0, H, H', Borrmann diffraction. (a) The intersection of the dispersion surface with the plane containing Laue point La, and the reciprocal-lattice points 0 and H. (b) A side view of (a) on the plane perpendicular to $0H$La.

more excited than Y_1. For a negative $S_{P,T}$, the excitation of the tie points has the same situation as that for a positive $S_{P,T}$.

In the experiment reported by Hart & Lang (1961), a variation on the two-beam and $2\bar{2}0$, *Pendellösung* fringe spacing due to the presence of the three-beam, $000\ 2\bar{2}0\ 3\bar{1}\bar{1}$, Borrmann diffraction was observed. For this three-beam case, $S_{P,T}$ is positive. The *Pendellösung* fringe spacing of two-beam diffraction is inversely proportional to the separation between the dispersion sheets. When the three-beam case with $S_{P,T} > 0$ comes into play, the fringe spacing at $\varphi < 0$ depends on the distance $X_1 X_2$ of the two strongly excited tie points. [Since the *Pendellösung* experiment involves an inclined crystal surface, the lines $Z_2 X_3$ and $W_2 Y_3$ (Fig. 1b) are tilted accordingly.] At $\varphi > 0$, the fringe spacing is inversely proportional to $Y_2 Y_3$. When the crystal surface is, for example, cut in such a way that lines $Z_2 X_3$ and $W_2 Y_3$ are parallel to the asymptotic line passing through Lo for branches 1 and 2 of Fig. 1(b), then

$$|X_1 X_2| < |L_1 L_3| < |Y_2 Y_3|. \tag{11}$$

$L_1 L_3$ is the separation between branches 1 and 2 for a two-beam H reflection. The inequality holds also for other inclined crystal surfaces. The $2\bar{2}0$ *Pendellösung* fringe spacing increased for $\varphi < 0$ and decreases for $\varphi > 0$. For a negative $S_{P,T}$, the situation is reversed. The theoretical ground on which the experiment (Hart & Lang, 1961) is based is correct. However, the method is impractical owing to the required wedge-shaped crystal, as long as the application to real crystal structure determination is concerned.

The divergent-beam photograph (Huang & Post, 1973) was used to provide phase information from the intensity distribution in the vicinity of a three-beam Borrmann diffraction point, in Post's (1977) experiment. The transmitted intensity of (9) depends not only on the term $D_T(j)$ related to the excitation, but also on the exponential term with the absorption from the imaginary part of $\mathbf{K}_T$ and with the sinusoidal crystal-thickness dependence from the real part of $\mathbf{K}_T$. According to Ewald & Heno (1968), the modes with dispersion sheets closest to the Laue point have the lowest absorption coefficients. By considering only the excitation of the mode and its absorption, the three-beam transmitted intensity for a negative $S_{P,T}$ shows the intensity asymmetry about the exact three-beam point, *i.e.* $\varphi = 0$. No intensity asymmetry is expected for a positive $S_{P,T}$. These facts are correctly discussed by Post (1977). However, that the sinusoidal term in (9) plays an important role in the transmitted intensity was not considered by Post (1977). In fact, the asymmetry of the transmitted intensity appears for thick crystals with $\mu t > 10$ (see, for example, Fig. 6, of Post, Chang & Huang, 1977). Even for $F_{\bar{1}\bar{1}1} F_{11\bar{1}} F_{002} = 0$ the intensity asymmetry occurs (see

Fig. 1 of Balter, Feldman & Post, 1971). For a thin crystal, absorption influences the transmitted intensity less. The sinusoidal term dominates the exponent of (9). The intensity asymmetry expected for a negative $S_{P,T}$ is smeared out by this sinusoidal variation, since the excitations of modes 1 and 3^+ for $\varphi < 0$ are almost equal to those of modes 2 and 3^+ for $\varphi > 0$ (Fig. 1b). It is clear that the crystal thickness effect outweighs the phase effect on the three-beam transmitted intensity. The use of the intensity distribution of three-beam Borrmann diffractions is therefore not well suited for phase determination.

(b) Two overlapped three-beam Umweg reflection and N-beam ($N > 3$) diffraction

The two overlapped *Umweg* reflections, $000\ 222\ 1\bar{1}\bar{1}$ and $000\ 222\ 111$ were treated as a four-beam case by Chapman, Yoder & Colella (1981) for phase determination. This case ought to be correctly treated as a five-beam case, since an additional $22\bar{2}$ reflection is closer to the $1\bar{1}\bar{1}$ reflection peak than the $1\bar{1}\bar{1}$ one. The coupling reflection is 004. Supposing that this additional three-beam, $000\ 222\ 22\bar{2}$, reflection is very weak, the overlapped case has been assumed as a four-beam case. The corresponding dispersion relation is equal to

$$\begin{pmatrix} \chi & F_{\bar{2}\bar{2}\bar{2}} & F_{\bar{1}11} & F_{\bar{1}1\bar{1}} \\ F_{222} & \chi & F_{133} & F_{131} \\ F_{1\bar{1}\bar{1}} & F_{\bar{1}\bar{3}\bar{3}} & \chi & F_{00\bar{2}} \\ F_{1\bar{1}1} & F_{\bar{1}\bar{3}\bar{1}} & F_{002} & \chi \end{pmatrix} = 0 \tag{12}$$

This equation involves many phase triplets and quartets. If one neglects the symmetry-related terms and treats the 002 as a forbidden reflection in spite of the asphericity of bonding electron in diamond structure (Ewald & Hönl, 1936), (12) still involves at least two phase triplets, $S_{\bar{2}\bar{2}\bar{2}} S_{1\bar{1}\bar{1}} S_{133}$ and $S_{\bar{2}\bar{2}\bar{2}} S_{1\bar{1}1} S_{131}$. The former is positive and the latter negative. It is very difficult to tell how the 222 reflected intensity would be influenced by these two phase triplets. The same argument can be applied to N-beam cases with $N > 3$. However, when the high-order phase products in these N-beam cases involve many symmetry-related reflections, these phase products can be expressed in terms of lower-order phase multiplets with $N \leq 3$. These N-beam cases can be, in principle, used for phase determination (Jagodzinski, 1980). Furthermore, when the N-beam cases with $N > 3$ involve many weak secondary and coupling reflections such that only a three-beam interaction dominates the whole diffraction process, these N-beam cases can then be treated as three-beam cases for phase determination.

(c) Three-beam Bragg reflection

From the analysis given above, three-beam Bragg reflections, either *Umweganregung* (Renninger, 1937)

or *Aufhellung* (Wagner, 1920), should be used for phase determinations, since the reflected intensity according to (8), is least affected by crystal thickness and since the dispersion surface is also directly related to the phase triplet. A practical experimental method for phase determination is given by Chang (1981, 1982). The situation whether the secondary reciprocal-lattice point is entering (incoming) or leaving (outgoing) the Ewald sphere is one of the two key facts which affect the intensity of multiple Bragg reflection, the other being the phase. The theoretical consideration of the relation between the dispersion surface and these two key facts is given in the following.

Fig. 2(a) is the 'projection' of the dispersion surface onto the 0*H*La plane. The dispersion sheets for the three-beam case involving a symmetric Bragg reflection *H* are schematically shown. Branches 1 and 2 are the dispersion sheets associated with the symmetric Bragg reflection. They represent the 0 and π phases for the wavefields inside the crystal. The region between branches 1 and 2 is the total reflection range. The horizontal axis, which is proportional to $\Delta\theta$, is denoted as $\Delta\theta$ in the same figure.

When the crystal is first set for the symmetric Bragg reflection *H*, the dispersion sheets, branches 1 and 2, are established. When the secondary reciprocal-lattice point then approaches the surface of the Ewald sphere, the starting point of K'_H moves along branch 3^+ for $S_{P,T} > 0$. The shape of the dispersion sheets 1 and 2 is modified by the presence of this additional reflection H'. At every angular setting, during the rotation of the secondary reciprocal-lattice point, the dispersion surface is excited by the incident X-ray beam at the tie points. For simplicity, the path of the moving $K_{H'}$ is projected on the $\Delta\theta$–φ plane, perpendicular to 0*H* (Fig. 2*b*), as the line *IJ*. The directions of motion, incoming and outgoing, are indicated in the same figure. The azimuthal angles at *I* and *J* are denoted as φ_m and φ_n. *M* and *N* in Fig. 2(*a*) are the entrance points on the crystal surface, corresponding to *I* and *J*. *MN* and *NP* are perpendicular to the crystal surface. It should be noticed that Fig. 2(*a*) is actually the combination of two intersections of the dispersion surface of φ_m and φ_n. Only the effective dispersion sheets are shown. For $\varphi = \varphi_m$, there are three tie points, *E*, *A*, and *B*, excited. Only the tie points *A* and *B*, whose Poynting vectors point towards the interior of the crystal, are effectively excited. Similarly, *C* and *G* are the two effective tie points at $\varphi = \varphi_n$. Since a tie point is the starting point for the propagation of the wavefield generated inside the crystal, the closer the two tie points are for a given φ, the stronger the dynamical interaction that takes place. Because *AB* is smaller than *CG*, strong interaction at φ_m generates a more intense diffracted beam towards the interior of the crystal than at φ_n. (The Poynting vectors at points *A*, *B*, *C*, and *G* point towards the reciprocal point 0.) For the conservation of total energy, the corresponding reflected intensity of the Bragg reflection *H* is therefore weaker at φ_m than at φ_n. This indicates that for a positive $S_{P,T}$ the reflected intensity on one side, $\varphi = \varphi_m$, of the multiple reflection peak (or dip), is lower than that on the other side, $\varphi = \varphi_n$. The situation is reversed if $S_{P,T}$ is negative or the diffraction is at its outgoing position.

Two *Umweg* reflections are considered as examples for illustration: (i) 000 222 1$\bar{1}\bar{1}$ with $S_{P,T}$ ($=S_{\bar{2}\bar{2}\bar{2}}S_{1\bar{1}\bar{1}}S_{133}$) > 0 and (ii) 000 222 113 with $S_{P,T}$ ($=S_{\bar{2}\bar{2}\bar{2}}S_{113}S_{11\bar{1}}$) < 0 of germanium for Cu $K\alpha_1$ radi-

(a)
Crystal Surface
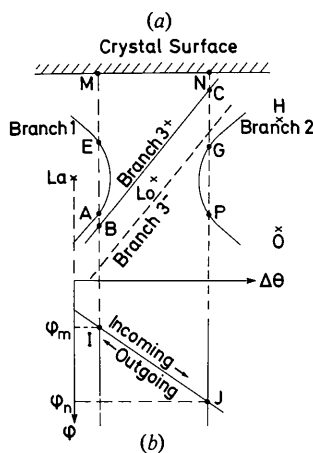
Fig. 2. Schematic representation of the dispersion surface for symmetric three-beam, 0, *H*, and *H'*, Bragg reflection. (*a*) The projection of the dispersion surface on the 0*H*La plane. (*b*) A bottom view of (*a*) on the plane perpendicular to 0*H*La.
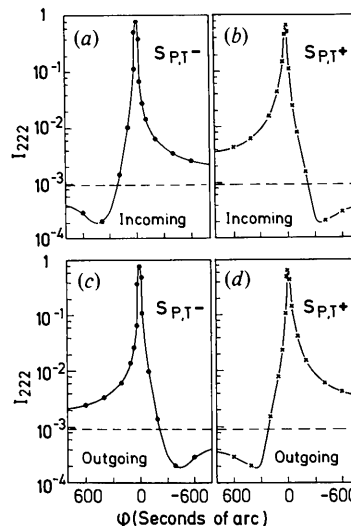

φ(Seconds of arc)

Fig. 3. Calculated germanium 222 reflected intensity profiles for the three-beam *Umweg*: 000 222 113, at the incoming (*a*) and the outgoing (*c*) situations; for the 000 222 1$\bar{1}\bar{1}$ case: at the incoming (*b*) and the outgoing (*d*) situations.

ation. The calculated intensity profiles obtained from (8) are shown in Fig. 3 for both cases at their incoming and outgoing positions. From these line profiles, the following relation is obtained for practical phase determination:

$$S_{P,E} = S_L \cdot S_R, \tag{13}$$

where $S_{P,E}$ is the experimentally determined sign of the phase triplet. S_L is the sign defined from the line profile. S_L is negative for the line profiles in Fig. 3(a) and (d). S_L is positive for the line profiles in Figs. 3(b) and (c). (Assume that the line profiles are recorded from the right side to the left side on a rolling chart.) S_R is determined from the sense of crystal rotation, either incoming or outgoing. By considering (7) and (8) of Cole, Chambers & Dunn (1962), S_R is defined as the sign of the derivative:

$$S_R = S\left(-\frac{\partial(1/\lambda)}{\partial\varphi}\right). \tag{14}$$

S_R is therefore positive for the incoming and negative for the outgoing situations.

Since multiple reflection patterns can be easily obtained by making a ψ scan on a four-circle single-crystal diffractometer, the sigh $S_{P,E}$ can be determined in a straight-forward manner from (13). There are, however, problems concerning its practical use, such as how to choose a proper primary reflection and the wavelength, and how to apply this method to mosaic crystals. Fortunately, the use of synchrotron provides an ideal means for solving these problems. On the other hand, conventional fine-focus X-ray tubes can also be employed to give reasonable conditions for the phase experiment if good crystals are used. Under these experimental conditions, a crystal structure, which could not be solved by the ordinary 'direct method', has been solved by using the present method. The results will be reported later (Han & Chang, 1982).

4. Conclusion

The analysis shows that three-beam multiple diffraction must be used for experimental determinations of phases. The difficulty of solving this phase problem experimentally is mainly because the crystal thickness dominates the diffracted intensity of three-beam Borrmann diffraction and that the rotation of the secondary reciprocal-lattice point relative to the Ewald sphere has not been considered properly, at least for X-rays. By considering this relative rotation and phase effects in three-beam Bragg reflections, a direct experimental method for the determination of X-ray reflection phases is obtained (Chang, 1981, 1982). There remain, however, many practical problems which ought to be solved for further application to real crystal structure determination.

References

BALTER, S., FELDMAN, R. & POST, B. (1971). Phys. Rev. Lett. 27, 307–309.
BATTERMAN, B. W. & COLE, H. (1964). Rev. Mod. Phys. 36, 681–717.
BERNDT, H. & DOLL, R. (1976). Optik (Stuttgart), 46, 309–332.
CHANG, S. L. (1979). Acta Cryst. A35, 543–547.
CHANG, S. L. (1981). Appl. Phys. A26, 221–226.
CHANG, S. L. (1982). Phys. Rev. Lett. 48, 163–166.
CHANG, S. L. & HAN, F.-S. (1982). Acta Cryst. A38, 414–417.
CHAPMANN, L. D., YODER, D. R. & COLELLA, R. (1981). Phys. Rev. Lett. 46, 1578–1580.
COLE, H., CHAMBERS, F. W. & DUNN, H. M. (1962). Acta Cryst. 15, 138–144.
COLELLA, R. (1974). Acta Cryst. A30, 413–423.
ECKSTEIN, H. (1949). Private communication to Lipscomb (1949).
EWALD, P. P. (1916a). Ann. Phys. (Leipzig), 49, 1–38.
EWALD, P. P. (1916b). Ann. Phys. (Leipzig), 49, 117–143.
EWALD, P. P. (1917). Ann. Phys. (Leipzig), 54, 519–556; 557–597.
EWALD, P. P. (1937). Z. Kristallogr. 97, 1–27.
EWALD, P. P. & HENO, Y. (1968). Acta Cryst. A24, 1–15.
EWALD, P. P. & HÖNL, H. (1936). Ann. Phys. (Leipzig), 25, 281–291.
FANKUCHEN, I. (1949). Private communication quoted by Lipscomb (1949).
HAN, F. S. & CHANG, S. L. (1982). In preparation.
HART, M. & LANG, A. R. (1961). Phys. Rev. Lett. 7, 120–122.
HUANG, T. C. & POST, B. (1973). Acta Cryst. A29, 35–37.
JAGODZINSKI, H. (1980). Acta Cryst. A36, 104–116.
JAMES, R. W. (1963). Solid State Phys. 15, 53–220.
KAMBE, K. (1957). J. Phys. Soc. Jpn, 12, 13–31.
KAMBE, K. & MIYAKE, S. (1954). Acta Cryst. 7, 216–218.
KATO, N. (1958). Acta Cryst. 11, 885–887.
KATO, N. (1974). In X-ray Diffraction, edited by L. V. AZAROFF. New York: McGraw-Hill.
KOHN, V. G. (1979). Phys. Status Solidi A, 54, 375–384.
LAUE, M. VON (1931). Ergeb. Exakten Naturwiss. 10, 133–158.
LAUE, M. VON (1960). Röntgentstrahl-Interferenzen. Frankfurt am Main: Akademische Verlag.
LIPSCOMB, W. N. (1949). Acta Cryst. 2, 193–194.
MADSEN, J. U. & COTTERILL, R. M. J. (1978). Acta Cryst. A34, 387–384.
MIYAKE, S. & KAMBE, K. (1954). Acta Cryst. 7, 218–220.
MOON, R. M. & SHULL, C. G. (1964). Acta Cryst. 17, 805–812.
PINSKER, Z. G. (1978). Dynamical Scattering of X-rays in Crystals. Berlin: Springer-Verlag.
POST, B. (1977). Phys. Rev. Lett. 39, 760–763.
POST, B., CHANG, S. L. & HUANG, T. C. (1977). Acta Cryst. A33, 90–97.
RENNINGER, M. (1937). Z. Phys. 106, 141–176.
SACCOCIO, E. J. & ZAJAC, A. (1965). Acta Cryst. 18, 478–480.
SCHWARTZ, L. H. & COHEN, J. B. (1977). Diffraction from Materials. New York: Academic Press.
WAGNER, E. (1920). Phys. Z. 21, 632, also quoted by Moon & Shull (1964).